

# RECONSIDERING EVALUATION PRACTICES IN MODULAR SYSTEMS: ON THE PROPAGATION OF ERRORS IN MRI PROSTATE CANCER DETECTION

Erlend Sortland Rolfsnes<sup>1‡</sup> Philip Thangngat<sup>1‡</sup>  
Trygve Eftestøl<sup>1</sup> Tobias Nordström<sup>2,3</sup> Fredrik Jäderling<sup>4,5</sup> Martin Eklund<sup>2</sup>  
Alvaro Fernandez-Quilez<sup>1,2,6†</sup>

<sup>1</sup>Department of Electrical Engineering and Computer Science, University of Stavanger, Norway.

<sup>2</sup>Department of Medical Epidemiology and Biostatistics, Karolinska Institutet, Sweden.

<sup>3</sup>Department of Molecular Medicine and Surgery, Karolinska Institutet, Sweden.

<sup>4</sup>Department of Radiology, Capio S:t Göran Hospital, Sweden.

<sup>5</sup>Department of Clinical Sciences, Danderyd Hospital, Karolinska Institutet, Sweden.

<sup>6</sup>SMIL, Department of Radiology, Stavanger University Hospital, Norway.

## ABSTRACT

Magnetic resonance imaging has evolved as a key component for prostate cancer (PCa) detection, substantially increasing the radiologist workload. Artificial intelligence (AI) systems can support radiological assessment by segmenting and classifying lesions in clinically significant (csPCa) and non-clinically significant (ncsPCa). Commonly, AI systems for PCa detection involve an automatic prostate segmentation followed by the lesion detection using the extracted prostate. However, evaluation reports are typically presented in terms of detection under the *assumption* of the availability of a highly accurate segmentation and an *idealistic* scenario, omitting the propagation of errors between modules. For that purpose, we evaluate the effect of two different segmentation networks (s1 and s2) with heterogeneous performances in the detection stage and compare it with an idealistic setting (s1:  $89.90 \pm 2.23$  vs  $88.97 \pm 3.06$  ncsPCa,  $P < .001$ ,  $89.30 \pm 4.07$  and  $88.12 \pm 2.71$  csPCa,  $P < .001$ ). Our results depict the relevance of a *holistic evaluation*, accounting for all the sub-modules involved in the system.

*Index Terms*— MRI, evaluation, prostate cancer, deep learning, detection

## 1. INTRODUCTION

Over the last decade, magnetic resonance imaging (MRI) has become an important tool for prostate cancer (PCa) detection, staging and treatment planning [1]. Its surge in relevance for PCa diagnosis is expected to substantially increase the amount of imaging examinations, and, consequently, the radiologist workload [2]. The increasing volume of MRI coupled with a shortage of specialists, presents a favorable scenario

to delegate time-consuming tasks such as segmentation of region of interests or detection of suspicious lesions to artificial intelligence (AI) systems [3, 4, 5].

The development of AI systems has seen a striking growth in the recent years. Recent developments are usually accompanied by empirical results showing their success in surpassing previous competitors in established benchmarks of tasks of proved difficulty [6, 7]. With the growth in task complexity, AI systems development has shifted to a *modular* approach [8]. Each module of the AI system is specialized and trained to achieve a high performance in each of the different *sub-tasks* with the ultimate goal of achieving a high performance in the *whole* system objective [3].

Whilst AI holds the potential to augment the radiologist abilities, reduce reader variability and shorten the study times, the increasing development and availability of AI software is not translated into clinical adoption [9, 10]. Some of the limitations and challenges for the adoption of AI systems in radiology practice are reported to stem from a *misalignment* between system characterization and the deployment scenario, where in the development phase, the evaluation of the AI system reports a high performance that does not match the one observed when deployed in clinical practice [9].

AI systems for PCa detection are, typically, systems that rely on two specialized *modules* [3]. As observed in Figure 1, the system is commonly composed of a module in charge of the automatic segmentation of the prostate from the MRI followed by a lesion detection module that depends on the quality of the segmented prostate. In spite of the dependence, the characterization of the system is generally performed under the *assumption* of the availability of a highly accurate prostate segmentation, hence providing an evaluation that only reflects the performance of the detection sub-system in an *idealized* setting [3, 11] and that might not be representative of the performance of the AI system as a *whole*.

‡ Equal contribution

† Corresponding author: alvaro.f.quilez@uis.no

## Training and validation

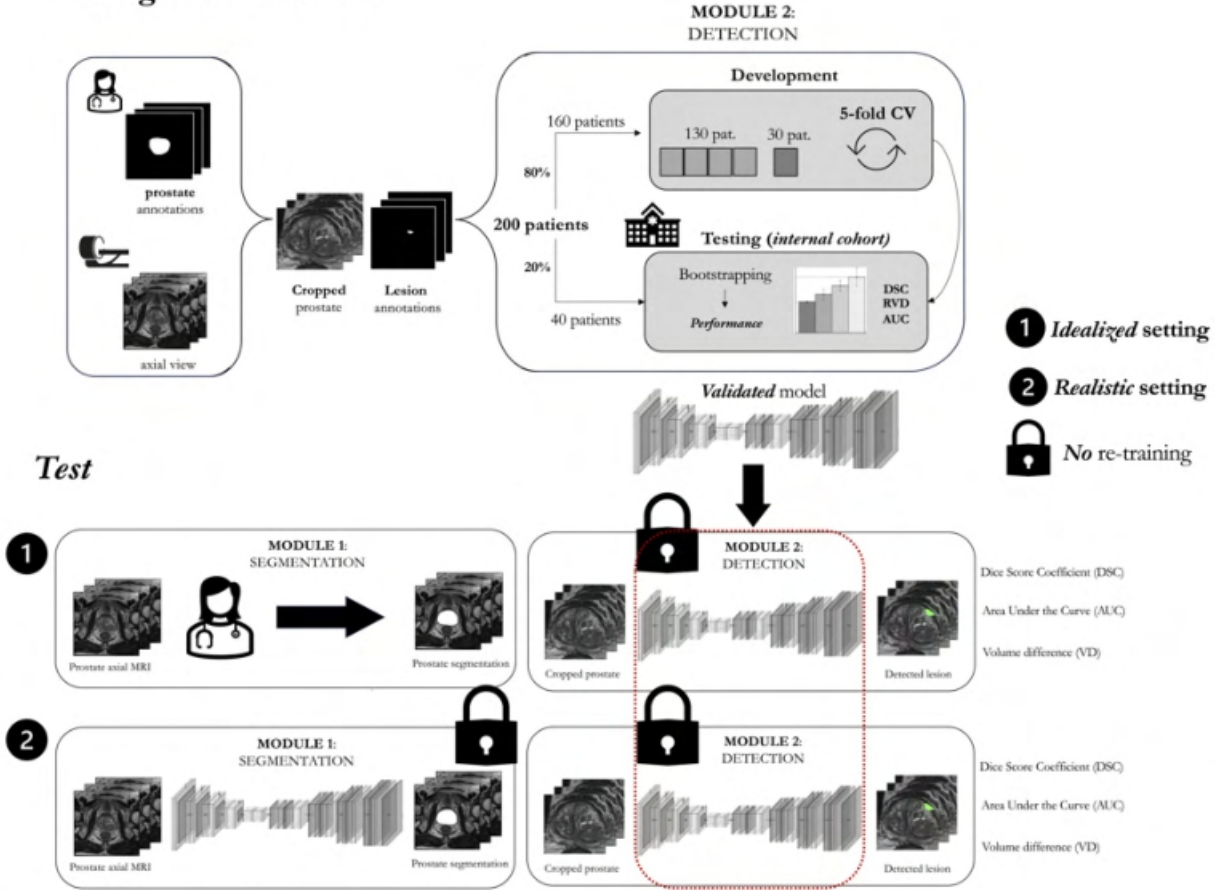


Fig. 1. Technical approach to the project including data selection, model development for PCa detection (tumor segmentation and classification), and testing phase in a realistic (and idealized) settings.

In this work, we aimed at evaluating the *effect of error propagation stemming from the prostate segmentation module in the performance of an AI-based PCa lesion detection system at test time*. For the remainder of the article, we refer to detection as the joint tasks of lesion segmentation and multi-class classification. For that purpose:

- We develop a PCa lesion detection system based on a U-Net [12] architecture that takes previously segmented prostates from MRI as an input.
- We test the detection system (i) under the assumption of a highly accurate prostate segmentation system (i.e. without errors, *idealized*).
- We test the detection system (i) using two previously developed highly accurate yet imperfect automatic AI systems to segment the prostate based on U-Net [4, 12] and nnU-Net [13, 14] (*realistic*).
- We evaluate and compare by means of statistical testing ( $P < .05$  significant) the *idealized* and *realistic* settings based on the PCa detection performance measured by the area under the curve (AUC) averaged values and

standard deviation (SD) obtained from  $n = 1000$  patient bootstrapped replicates without repetition.

## 2. METHODS

### 2.1. Data

A total of 200 patients (median age 66 years [range, 48-83 years]; men) from the publicly available ProstateX dataset [15] served as the main source for model *development* and *testing*. Patients considered for the study were initially screened for PCa based on prostate specific antigen levels and MRI scoring. Patients with confirmed cancer diagnosis through a MRI-guided biopsy were included in the study.

Patients' lesions with gleason scores (GS)  $\geq 7$  were classified as clinically-significant (csPCa), whilst lesions with GS  $\leq 6$  as non-clinically significant (ncsPCa).

T2-weighted (T2w) axial sequences were considered the main imaging data source. The acquisition was performed with a 3.0-Tesla (T) Siemens scanner with an in-plane resolution of 0.5 x 0.5 mm, 3.6 mm slice thickness and with a sur-

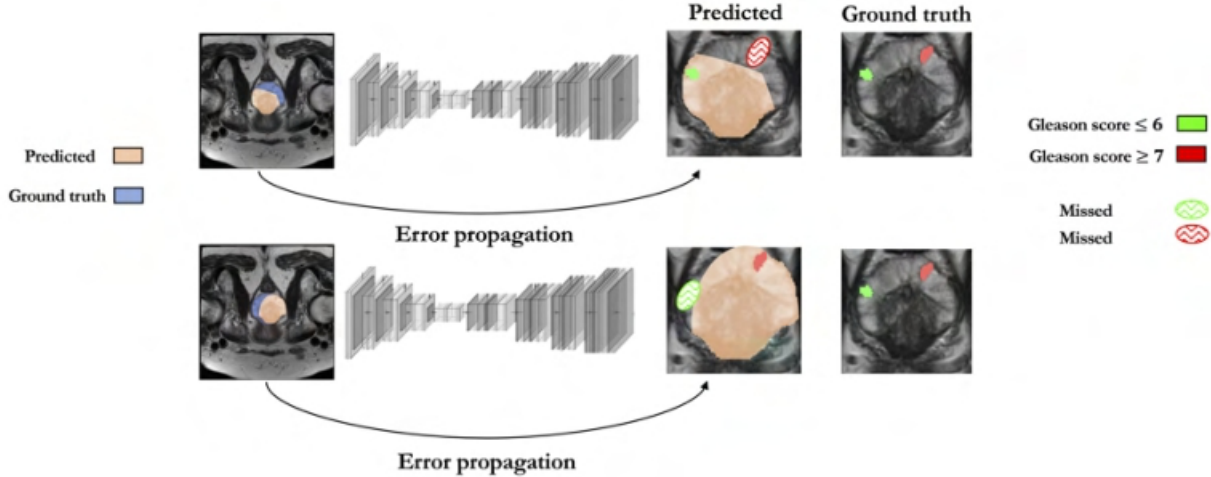


Fig. 2. Error propagation and subsequent missed lesion segmentation due to a faulty prostate segmentation.

face coil [14]. Binary pixel-level manual annotations of the prostate and the lesions were performed by two radiologists in-training and two experienced board-certified radiologists [16].

### 2.1.1. Pre-processing and data splitting

To have a common space of reference, we apply a re-sampling by linear interpolation to all the T2w sequences to a resolution of  $0.5 \times 0.5 \times 3.6$  mm followed by N4 bias field correction filtering, and a normalization of the pixel intensity of the sequences [17]. To obtain multi-class pixel-level lesion segmentations, we collapsed both masks and assigned a unique class to pixels belonging to background, ncsPCa and csPCa lesions, as depicted in Figure 2. Finally, we one-hot encode the masks.

We split the data avoiding cross-contamination in 80/20% to obtain the train and test set, resulting in 160 and 40 patients, respectively. The splitting is performed in a stratified way, which results in 498 (69.17% of the total) ncsPCa lesions in the train set, 186 (67.88%) in the test set, 222 (30.83%) csPCa lesions in the train set and 88 (32.12%) in the test set.

## 2.2. Bi-modular system: prostate segmentation and lesion detection

The whole detection system is composed of two modules: automatic prostate segmentation [4, 13] and lesion detection (Figure 1). Development of the automatic prostate segmentation module is considered out of the scope of the work. Hence, in the remaining of the paper we leverage two *existing* models trained and tested with the same splits as the ones used to develop the lesion detection sub-module. In particular, we focus on a previously reported multi-view segmentation network [4] and a standard nn-UNet [13, 14].

### 2.2.1. Lesion detection: implementation and training

We adopt a standard U-Net architecture [12], with the addition of dropout blocks with probability  $p = 0.15$  in the last two blocks of the encoder and two first blocks of the decoder to avoid overfitting. We use an ImageNet pre-trained model and a channel-wise convolutional block to map the original gray-scale images (1 channel) to the expected Red-Green-Blue (RGB) format (3 channels). We apply standard image augmentations at training time: horizontal flip, rotation ( $[-70, 70]$  degrees) and translation along the x-axis. All augmentations are implemented with probability  $p = 0.5$ .

The architecture is *trained* using T2w slices (2D) as an input, with a multi-class dice score loss, Adam optimizer and for 90 epochs. All the aforementioned augmentations are applied *on the fly*. The training is performed with a 5-fold cross-validation (CV). The model is implemented using Tensorflow and Python language. We train and evaluate the model on an NVIDIA A100 GPU.

### 2.2.2. Error propagation: impact on lesion detection

We evaluate the impact of error propagation from the segmentation module to the detection module *at test time*. That is, when training the detection module, we *assume an ideal* setting in which both human-annotated prostate masks and lesion masks are available. We note that at testing time, both modules are intended to operate with as less human intervention as possible. Hereby, we devise two scenarios to quantify the impact of an imperfect prostate annotation at test time:

- We use the original expert-annotated prostate masks to crop the prostate from the T2w corresponding sequence. Following, we quantify the detection ability of the lesion detection module in an ideal setting, where no AI errors are propagated between sub-modules.
- We use the automatically AI-generated prostate masks to

Setting	Prostate segmentation			Module				
	Architecture	DSC (%) $\uparrow$	VD (%) $\downarrow$	Tumor	DSC (%) $\uparrow$	VD (%) $\downarrow$	AUC (%) $\uparrow$	$p_{AUC}^\dagger$
Idealized	-	-	-	ncsPCa	25.97 $\pm$ 1.34	4.09 $\pm$ 3.46	89.90 $\pm$ 2.23	-
	-	-	-	csPCa	15.40 $\pm$ 1.96	0.38 $\pm$ 0.25	89.30 $\pm$ 4.07	-
Realistic	nnU-Net (s1) [13]	97.10 $\pm$ 0.22	-0.01 $\pm$ 0.12	ncsPCa	25.08 $\pm$ 1.85	4.93 $\pm$ 2.57	88.97 $\pm$ 3.06	<.001 $^\ddagger$
	tU-Net (s2) [4]	90.07 $\pm$ 0.74	2.01 $\pm$ 1.30	csPCa	12.24 $\pm$ 3.01	2.93 $\pm$ 2.41	88.12 $\pm$ 2.71	<.001 $^\ddagger$
				ncsPCa	23.84 $\pm$ 0.98	4.86 $\pm$ 3.72	83.57 $\pm$ 3.61	<.001 $^\ddagger$
				csPCa	10.14 $\pm$ 2.05	3.08 $\pm$ 2.96	81.30 $\pm$ 3.83	<.001 $^\ddagger$

$^\dagger$  Reference is *Idealized* setting results.

$^\ddagger$  Statistically significant.

Table 1. Results at the patient level for lesion detection in idealized and realistic settings.

crop the prostate from the T2w corresponding sequence, regardless of the error associated to that prostate mask. Following, we quantify the detection ability of the lesion detection module. We repeat the process for two different prostate segmentation architectures (s1 and s2) with different reported performances at test time.

### 2.3. Evaluation

We provide an evaluation at the *patient level* based on the lesion segmentation and classification performance of the lesion detection sub-module. Results are presented as mean $\pm$ standard deviation (SD) for Dice Score Coefficient (DSC, %) and Volume Difference (VD, %) to characterize the segmentation of the lesion. We refer to the same metrics [14], if necessary, to characterize the segmentation of the prostate. We use area under the curve (AUC) to characterize the *per class* lesion detection ability (csPCa and ncsPCa). We estimate the variability of the results using a non-parametric bootstrapping with  $n = 1000$  replicates without repetition. We assess statistical significance at the  $P \leq .05$  level for AUC using permutation tests.

#### 2.3.1. From lesion segmentation to classification

Lesions sharing a minimum DSC of 0.10 when compared with the ground truth were considered true positives. We follow a similar choice to the one presented in previous works [3], with the underlying rationale that the majority of lesions are small (<2cm<sup>3</sup>) and hence, a relatively small overlap in DSC can be considered as a successful detection of the lesion.

## 3. RESULTS

Table 1 presents the main results for the error propagation assessment between the prostate segmentation module and the lesion detection one, from an *idealized* and *realistic* perspective. After applying a threshold of DSC  $\geq 10.00\%$  to

the lesion segmentation in the *idealized* setting, the detection system reaches an AUC of 89.90  $\pm$  2.23 for ncsPCa lesions and an AUC of 89.30  $\pm$  4.07 for csPCa. When assessing the detection in the *realistic* setting, we observe a significantly lower performance when compared to the *idealized* setting: 88.97  $\pm$  3.06 ncsPCa  $P < .001$ ) and 88.12  $\pm$  2.71 csPCa  $P < .001$ , nnUNet (s1) and 83.57  $\pm$  3.61 ncsPCa  $P < .001$  and 81.30  $\pm$  3.83 csPCa,  $P < .001$ , tUNet (s2).

## 4. DISCUSSION

Traditionally, the evaluation of modular systems is carried out without accounting for the error propagation between the sub-modules. In our study, we observe that even a highly accurate nnUNet segmentation module [14] can still produce results that can result catastrophic for the purpose of the tumor segmentation and classification (Table 1). The effect of the mistakes in these segmentation module become more noticeable when using a lesser accurate prostate segmentation architecture, tUNet [4]. Our results show the relevance of accounting for small errors at the individual module level that can propagate and result in big errors in the context of the global system in prostate cancer detection.

## 5. CONCLUSIONS

Our study depicts the importance of holistic evaluations in prostate cancer detection modular systems, accounting for error propagation between modules and avoiding significant performance degradation.

## 6. COMPLIANCE WITH ETHICAL STANDARDS

Ethical approval was not required as confirmed by the license attached with the public data.

## 7. ACKNOWLEDGMENTS

The authors have no relevant financial or non-financial interests to disclose.

## 8. REFERENCES

- [1] Martin Eklund, Fredrik Jäderling, Andrea Discacciati, Martin Bergman, Magnus Annerstedt, Markus Aly, Axel Glaessgen, Stefan Carlsson, Henrik Grönberg, and Tobias Nordström, “Mri-targeted or standard biopsy in prostate cancer screening,” *New England Journal of Medicine*, vol. 385, no. 10, pp. 908–920, 2021.
- [2] Alvaro Fernandez-Quilez, Tobias Nordström, Fredrik Jäderling, Svein Reidar Kjosavik, and Martin Eklund, “Prostate age gap (pag): An mri surrogate marker of aging for prostate cancer detection,” *arXiv preprint arXiv:2308.05344*, 2023.
- [3] Anindo Saha, Matin Hosseinzadeh, and Henkjan Huisman, “End-to-end prostate cancer detection in bpmri via 3d cnns: effects of attention mechanisms, clinical priors and decoupled false positive reduction,” *Medical image analysis*, vol. 73, pp. 102155, 2021.
- [4] Tim Nikolass Lindeijer, Tord Martin Ytredal, Trygve Eftestøl, Tobias Nordström, Fredrik Jäderling, Martin Eklund, and Alvaro Fernandez-Quilez, “Leveraging multi-view data without annotations for prostate mri segmentation: A contrastive approach,” *arXiv preprint arXiv:2308.06477*, 2023.
- [5] Andrés Anaya-Isaza, Leonel Mera-Jiménez, and Alvaro Fernandez-Quilez, “Crosstransunet: A new computationally inexpensive tumor segmentation model for brain mri,” *IEEE Access*, vol. 11, pp. 27066–27085, 2023.
- [6] Biyang Guo, Xin Zhang, Ziyuan Wang, Minqi Jiang, Jinran Nie, Yuxuan Ding, Jianwei Yue, and Yupeng Wu, “How close is chatgpt to human experts? comparison corpus, evaluation, and detection,” *arXiv preprint arXiv:2301.07597*, 2023.
- [7] Karan Singhal, Tao Tu, Juraj Gottweis, Rory Sayres, Ellery Wulczyn, Le Hou, Kevin Clark, Stephen Pfohl, Heather Cole-Lewis, Darlene Neal, et al., “Towards expert-level medical question answering with large language models,” *arXiv preprint arXiv:2305.09617*, 2023.
- [8] Yann LeCun, “A path towards autonomous machine intelligence version 0.9. 2, 2022-06-27,” *Open Review*, vol. 62, 2022.
- [9] Kasumi Widner, Sunny Virmani, Jonathan Krause, Jay Nayar, Richa Tiwari, Elin Rønby Pedersen, Divleen Jeji, Naama Hammel, Yossi Matias, Greg S Corrado, et al., “Lessons learned from translating ai from development to deployment in healthcare,” *Nature Medicine*, pp. 1–3, 2023.
- [10] Anna Kurbatskaya, Alberto Jaramillo-Jimenez, John Fredy Ochoa-Gomez, Kolbjørn Brønnick, and Alvaro Fernandez-Quilez, “Assessing gender fairness in eeg-based machine learning detection of parkinson’s disease: A multi-center study,” *arXiv preprint arXiv:2303.06376*, 2023.
- [11] Nils Netzer, Carolin Eith, Oliver Bethge, Thomas Hielscher, Constantin Schwab, Albrecht Stenzinger, Regula Gnirs, Heinz-Peter Schlemmer, Klaus H Maier-Hein, Lars Schimmöller, et al., “Application of a validated prostate mri deep learning system to independent same-vendor multi-institutional data: demonstration of transferability,” *European Radiology*, pp. 1–14, 2023.
- [12] Olaf Ronneberger, Philipp Fischer, and Thomas Brox, “U-net: Convolutional networks for biomedical image segmentation,” in *Medical Image Computing and Computer-Assisted Intervention—MICCAI 2015: 18th International Conference, Munich, Germany, October 5-9, 2015, Proceedings, Part III 18*. Springer, 2015, pp. 234–241.
- [13] Fabian Isensee, Paul F Jaeger, Simon AA Kohl, Jens Petersen, and Klaus H Maier-Hein, “nnu-net: a self-configuring method for deep learning-based biomedical image segmentation,” *Nature methods*, vol. 18, no. 2, pp. 203–211, 2021.
- [14] Alvaro Fernandez-Quilez, Tobias Nordstom, Trygve Eftestøl, Andreas Bremset Alvestad, Fredrik Jaderling, Svein Reidar Kjosavik, and Martin Eklund, “Revisiting prostate segmentation in magnetic resonance imaging (mri): On model transferability, degradation and pirads adherence,” *medRxiv*, pp. 2023–08, 2023.
- [15] Geert Litjens, Oscar Debats, Jelle Barentsz, Nico Karssemeijer, and Henkjan Huisman, “Computer-aided detection of prostate cancer in mri,” *IEEE transactions on medical imaging*, vol. 33, no. 5, pp. 1083–1092, 2014.
- [16] Renato Cuocolo, Albert Comelli, Alessandro Stefano, Viviana Benfante, Navdeep Dahiya, Arnaldo Stanzione, Anna Castaldo, Davide Raffaele De Lucia, Anthony Yezzi, and Massimo Imbriaco, “Deep learning whole-gland and zonal prostate segmentation on a public mri dataset,” *Journal of Magnetic Resonance Imaging*, vol. 54, no. 2, pp. 452–459, 2021.
- [17] Alvaro Fernandez-Quilez, Trygve Eftestøl, Svein Reidar Kjosavik, Morten Goodwin, and Ketil Oppedal, “Contrasting axial t2w mri for prostate cancer triage: A self-supervised learning approach,” in *2022 IEEE 19th International Symposium on Biomedical Imaging (ISBI)*, 2022, pp. 1–5.